



Contents lists available at ScienceDirect

Mechanisms of Development

journal homepage: www.elsevier.com/locate/mod

Probing the kinetic landscape of Hox transcription factor–DNA binding in live cells by massively parallel Fluorescence Correlation Spectroscopy

Dimitrios K. Papadopoulos^{a,*}, Aleksandar J. Krmpot^{b,c,1}, Stanko N. Nikolić^{b,c}, Robert Krautz^d, Lars Terenius^b, Pavel Tomancak^a, Rudolf Rigler^{e,f}, Walter J. Gehring^{g,2}, Vladana Vukojević^{b,*}

^a Max-Planck Institute for Molecular Cell Biology and Genetics, 01307 Dresden, Germany

^b Department of Clinical Neuroscience (CNS), Center for Molecular Medicine (CMM), Karolinska Institutet, 17176 Stockholm, Sweden

^c Institute of Physics, University of Belgrade, 11080 Belgrade, Serbia

^d Department of Molecular Biosciences, The Wenner-Gren Institute, Stockholm University, 10691 Stockholm, Sweden

^e Department of Medical Biochemistry and Biophysics, Karolinska Institutet, 17177 Stockholm, Sweden

^f Laboratory of Biomedical Optics, Swiss Federal Institute of Technology, 1015 Lausanne, Switzerland

^g Department of Cell Biology, Biozentrum, University of Basel, 4056 Basel, Switzerland

ARTICLE INFO

Article history:

Received 16 March 2015

Received in revised form 23 September 2015

Accepted 24 September 2015

Available online xxxx

Keywords:

Hox genes

Sex combs reduced

Dimer formation

Massively parallel Fluorescence Correlation Spectroscopy

Bimolecular Fluorescence Complementation

Transcription factor–DNA binding

ABSTRACT

Hox genes encode transcription factors that control the formation of body structures, segment-specifically along the anterior–posterior axis of metazoans. Hox transcription factors bind nuclear DNA pervasively and regulate a plethora of target genes, deploying various molecular mechanisms that depend on the developmental and cellular context. To analyze quantitatively the dynamics of their DNA-binding behavior we have used confocal laser scanning microscopy (CLSM), single-point fluorescence correlation spectroscopy (FCS), fluorescence cross-correlation spectroscopy (FCCS) and bimolecular fluorescence complementation (BiFC). We show that the Hox transcription factor Sex combs reduced (Scr) forms dimers that strongly associate with its specific *fork head* binding site (*fh250*) in live salivary gland cell nuclei. In contrast, dimers of a constitutively inactive, phosphomimicking variant of Scr show weak, non-specific DNA-binding. Our studies reveal that nuclear dynamics of Scr is complex, exhibiting a changing landscape of interactions that is difficult to characterize by probing one point at a time. Therefore, we also provide mechanistic evidence using massively parallel FCS (mpFCS). We found that Scr dimers are predominantly formed on the DNA and are equally abundant at the chromosomes and an introduced multimeric *fh250* binding-site, indicating different mobilities, presumably reflecting transient binding with different affinities on the DNA. Our proof-of-principle results emphasize the advantages of mpFCS for quantitative characterization of fast dynamic processes in live cells.

© 2015 Elsevier Ireland Ltd. All rights reserved.

Introduction

Hox transcription factors specify segmental identity in animals by launching the developmental programs required for morphological diversification of segments, such as the formation of body appendages and the acquisition of specialized functions (Gehring, 1987; Lewis, 1978; McGinnis and Krumlauf, 1992). However, despite the wealth of knowledge on their biological function, we still lack detailed mechanistic insight into how they achieve their complex function *in vivo*, at the molecular level.

The DNA-binding properties of Hox transcription factors in large metazoan genomes, and the mechanisms deployed thereby to control the regulation of their target genes, remain open questions in developmental biology. The dynamic behavior of Hox transcription factors in the nucleus can be viewed in its entirety as the problem of Hox specificity, namely how Hox transcription factors, that are structurally very similar in their DNA-binding preferences and bind in a widespread manner in the genome, regulate apparently dissimilar morphogenetic programs, such as the formation of body appendages, as diverse as a fly wing and an antenna. In *Drosophila*, a wealth of studies has approached the problem of Hox specificity, either structurally or functionally.

Structural studies of homeodomain–DNA binding are exemplified in the context of Scr (Joshi et al., 2007), Ultrabithorax (Ubx) (Passner et al., 1999) and Antennapedia (Antp) (Muller et al., 1988; Otting et al., 1990; Otting et al., 1988; Qian et al., 1989), for which the corresponding DNA-bound structures have been resolved by X-ray crystallography or NMR, respectively. In these structures, DNA binding topologies have been

* Corresponding authors.

E-mail addresses: papadopo@mpi-cbg.de (D.K. Papadopoulos),

vladana.vukojevic@ki.se (V. Vukojević).

¹ These authors contributed equally to this work.

² We are deeply saddened by the sudden loss of our colleague Prof. Walter J. Gehring, a visionary scientist whose work will continue to educate and inspire many generations to come. This work is devoted to his memory.

<http://dx.doi.org/10.1016/j.mod.2015.09.004>

0925-4773/© 2015 Elsevier Ireland Ltd. All rights reserved.

Please cite this article as: Papadopoulos, D.K., et al., Probing the kinetic landscape of Hox transcription factor–DNA binding in live cells by massively parallel Fluorescence Correlati..., Mechanisms of Development (2015), <http://dx.doi.org/10.1016/j.mod.2015.09.004>

mapped to the third helix of the homeodomain (major DNA groove contacts), as well as its N-terminal arm sequences (minor DNA groove contacts). Careful examination of these structures, as in the case of Antp, has identified important roles of the N-terminal arm of the homeodomain (Qian et al., 1994) and the linker between the YPWM motif (also termed the hexapeptide motif) and the homeodomain (Qian et al., 1992) in DNA-binding affinities. In fact, both the YPWM motif and the N-terminal arm of the homeodomain have been found to play a major role in specificity (Papadopoulos et al., 2011; Papadopoulos et al., 2012; Papadopoulos et al., 2010). Such specificity, as in the cases of Scr and Antp, is required for paralog specific functions (Furukubo-Tokunaga et al., 1993; Gibson et al., 1990; Zeng et al., 1993), although the structure of the *cis*-binding site (the structure of the DNA minor groove itself) is equally important for target recognition, at least in the cases of Scr and Deformed (Dfd) (Joshi et al., 2007; Joshi et al., 2010).

Functional studies on the specificity of Hox proteins have led to the identification of cofactors, which physically interact with Hox transcription factors and allow the binding of Hox complexes with higher stringency on the DNA. For example, Extradenticle (Exd) binds DNA together with Hox proteins, interacts physically with them *via* the YPWM motif and functions as a generic Hox cofactor (Mann and Chan, 1996). The contribution of Exd in Hox function can be appreciated, for instance, in the case of determination of antennal and leg identities (Casares and Mann, 1998), or salivary gland morphogenesis (Rieckhof et al., 1997), which depends on the regulation of the *fkf* gene, and which, in turn, represents one of the extensively characterized *bona fide* targets of Scr (Ryoo and Mann, 1999). Moreover, the YPWM motif and its interaction with cofactors have been remarkably conserved in evolution, emphasizing their importance in Hox functionality (Chang et al., 1995; Knoepfler and Kamps, 1995; Lu et al., 1995).

Notwithstanding the validity of such studies in elucidating the function and specificity of Hox factors, little quantitative information has been gained. We still do not know how much transcription factor is contained in cells, how often and how strongly it binds to the DNA, how long it stays on the DNA, as well as how other transcription factors/cofactors/interacting proteins are embedded into Hox reaction–diffusion networks to control the dynamics and kinetics of DNA-binding and, thereby, gene regulation. As with most biomolecules, the temporal evolution and spatial distribution of transcription factors in live cell nuclei are the most important determinants of their kinetic behavior. Despite this, comprehensive quantitative information on the cellular dynamics of molecules in these processes is still lacking. The importance of the kinetics of Hox–DNA binding has been appreciated already in early studies (Affolter et al., 1990). To date, technological advances have allowed the quantification of transcription factors with high precision, at least *ex vivo* (Simicevic et al., 2013). Few attempts have been made to dissect the dynamics of Hox–DNA binding behavior using methods that allow the quantification of concentration and molecular mobility in live cells, such as single-point FCS (Gehring, 2011; Vukojevic et al., 2010). These studies outlined the importance of the measurement of transcription factor behavior in live cells, but could not study this behavior simultaneously in a heterogeneous system, such as a whole cell nucleus or cells in a larger tissue.

In this paper we utilize a prototype instrument for mpFCS measurements that is developed in our laboratory (Vitali et al., 2014 and Krmpot et al., in preparation) to study *in vivo* the integration of Scr transcription factor molecules into reaction–diffusion networks in the nuclei of giant salivary gland polytene cells, a tissue that is normally specified by Scr during development.

Scr is expressed in the labial and prothoracic segments of the embryo (Kuroiwa et al., 1985; LeMotte et al., 1989; Martinez-Arias et al., 1987), the central nervous system and subesophageal ganglia (Mahaffey and Kaufman, 1987), as well as predominantly in the prothoracic, among the larval, imaginal discs (Glücksman et al., 1987). In these primordia, Scr specifies prothoracic leg development, while being – at

least in part – responsible for repression of prothoracic wing formation (Rogers et al., 1997), a function conserved across extant insects (Hrycaj et al., 2010). Scr has been functionally preserved in evolution, which is best demonstrated by the ability of its mouse ortholog to induce Scr-specific homeotic transformations in flies (Zhao et al., 1993; Zhao et al., 1996). Finally, Scr plays a pivotal role in the specification of salivary gland development (Andrew et al., 1994; Panzer et al., 1992; Zhou et al., 2001).

Here, we make use of flies expressing wild-type or constitutively inactive Scr variants. They also carry a 50mer of the *fkf250* specific binding site (Ryoo and Mann, 1999), to which Scr dimers bind strongly and accumulate in salivary gland cells (Papadopoulos et al., 2012). Our experimental setup allows us to quantitatively characterize the spatial distribution of Scr molecules and measure differences in their local diffusion properties across the whole cell nucleus.

Materials and methods

Microscopic setups

The ConfoCor 3 instrument and a prototype microscopic setup for mpFCS, have been used in this study.

The uniquely modified ConfoCor3 instrument (Carl Zeiss, Jena, Germany) consisting of an inverted microscope for transmitted light and epifluorescence (Axiovert 200 M); a vis–laser module comprising the Ar/ArKr (458, 477, 488 and 514 nm), HeNe 543 nm and HeNe 633 nm lasers; and the scanning module LSM 510 META was used for single-point measurements. The instrument is modified to enable detection using silicon Avalanche Photo Detectors (SPCM-AQR-1X; PerkinElmer, USA) for imaging, which allows confocal fluorescence microscopy imaging with single-molecule sensitivity (Vukojevic et al., 2008). Images were recorded at a 512 × 512 pixel resolution. The C-Apochromat 40×/1.2 W UV-VIS-IR objective was used throughout. Fluorescence intensity fluctuations were recorded in arrays of 10–30 consecutive measurements, each measurement lasting 5–10 s. Averaged curves were analyzed using the software for online data analysis or exported and fitted offline using the OriginPro 8 data analysis software (OriginLab Corporation, Northampton, MA). In either case, the nonlinear least square fitting of the autocorrelation curve was performed using the Levenberg–Marquardt algorithm. Quality of the fitting was evaluated by visual inspection and by residuals analysis.

The specific design and construction of the mpFCS setup is described elsewhere (Vitali et al., 2014 and Krmpot et al., in preparation). Briefly, simultaneous excitation of fluorescent molecules across the specimen is achieved by passing a single laser beam through a diffractive optical element (DOE), which transforms it into a rectangular illumination matrix that consists of 32 × 32 spots. Fluorescence from 1024 illuminated spots is detected in a confocal arrangement by a matching matrix detector consisting of the same number of single-photon avalanche photodiodes (SPADs). Dedicated software was developed for data acquisition and fast auto- and cross-correlation analysis by parallel signal processing using a graphic processing unit (GPU). This approach enables quantitative characterization of physiological processes in live cells/tissue with a sub-millisecond temporal resolution, presently 21 μs/frame. The prototype setup also allows single-molecule sensitivity, but for long signal acquisition times. Due to technical limitations, such measurements are presently feasible only if the number of pixels is being reduced.

Expression of Scr transcription factors in *Drosophila* salivary glands

Expression of UAS-mCitrine-Scr(wt) alone, or of combinations of UAS-mCitrine-Scr(wt) and UAS-mCherry-Scr(wt), as well as UAS-mCitrine-Scr(DD) and UAS-mRFP1-Scr(DD), has been induced by *dpp^{blk}*-Gal4 (Staebling-Hampton et al., 1994), or *sgs3*-Gal4 (obtained from the Bloomington Stock Center, stock number 6870). The 50mer of

fkh250 binding sites is bound by Scr homodimers and has been previously described (Papadopoulos et al., 2012). Fluorescent balancers (Le et al., 2006) and examination of salivary gland fluorescence through the larval cuticle have been used for selection of genotype.

Expression of Scr dimers by bimolecular fluorescence complementation (BiFC) in *Drosophila* salivary glands

Flies expressing synthetic UAS- V_C -Scr and UAS- V_N -Scr constructs, as wild-type or constitutively inactive variants, have been used in this study, as previously described (Papadopoulos et al., 2012; Papadopoulos et al., 2010). The synthetic Scr constructs are comprised of the homeodomain, YPWM motif and C-terminus, tagged to the C (V_C) or N (V_N) terminus of the Venus fluorescent protein and they successfully recapitulate the Scr homeotic function to a great extent (Papadopoulos et al., 2012). Expression has been induced using the *sgs3*-Gal4 driver. Fluorescent balancers (Le et al., 2006) and examination of salivary gland fluorescence through the larval cuticle have been used for selection of genotype.

Preparation of salivary glands for live measurements

Salivary glands of third instar larvae have been dissected in phosphate buffered saline (PBS) at room temperature and transferred to 8-well chambered cover glass (Nunc® Lab-Tek® II, Thermo Fisher Scientific, USA) containing 200 μ L of PBS. Salivary glands were then used directly for measurements.

Results

We have previously used single-point FCS to quantitatively characterize the complex Scr DNA-binding in live salivary gland cell nuclei (Vukojevic et al., 2010). However, the transcription factor molecules are not uniformly distributed in polytene nuclei (Fig. 1). They undergo free-diffusion in the nucleoplasm (Fig. 1A, blue circle), bind to chromosomal DNA, both specifically and non-specifically (Fig. 1A, green circle), and form sites of accumulation on the DNA (Fig. 1A, red circle). This suggests that Scr participates in different types of interactions in the nucleus at different locations. In classical, single-point FCS, fluorescence intensity fluctuations in a stationary observation volume element (OVE) are recorded over time, using detectors with single-photon

sensitivity, and subjected to autocorrelation analysis, which provides information about the average number of fluorescent molecules in the OVE and their mobility. (For an overview of FCS methodology, refer to Vukojevic et al., 2005). FCS measurements on the aforementioned nuclear locations reveal differences in mobility between the nucleoplasm and the polytene chromosomes (Fig. 1B). These are evident from the shift of the autocorrelation curve (ACC) recorded in the nucleoplasm towards shorter decay times, as compared to the ACC recorded on the polytene chromosomes and at the site of accumulation, where longer decay time is observed, indicating binding to the DNA (Fig. 1B, blue versus red ACCs). However, little – if any – difference in molecular mobility is observed between the sites of high Scr concentration and its binding elsewhere on the chromosomes (Fig. 1B, compare green and red FCS curves). Moreover, the strong fluorescence intensity observed at Scr binding sites in the nucleus suggests that, in addition to Scr accumulation, higher order complexes are formed on the DNA.

We have previously established that Scr forms homodimers, which are required for a great portion of its homeotic function in flies (Papadopoulos et al., 2012). Here, we have sought to characterize the DNA binding behavior of these dimers using the BiFC system (Hu et al., 2002) and FCS.

In BiFC, proteins that are hypothesized to interact are tagged to the N- and C-terminal portions (V_N and V_C , respectively) of the Venus fluorescent protein. While the two halves of Venus do not fluoresce on their own, when the two interacting partners bring them together, fluorescence is being reconstituted. BiFC has been successfully used in many systems, including flies, for monitoring protein–protein interactions, as in the case of Hox transcription factors and their interacting partners (Boube et al., 2014; Duffraisse et al., 2014; Hudry et al., 2014; Hudry et al., 2011; Papadopoulos et al., 2012; Sambrani et al., 2013).

By CLSM, we have observed that Scr dimers reside overwhelmingly on the DNA (Fig. 2A) and accumulate on chromosomal regions of decondensed chromatin (polytene chromosome interbands). In contrast, a constitutively inactive phosphomimicking variant of Scr, where threonine 6 and serine 7 of the homeodomain have been substituted by aspartates [Scr(DD)] (Berry and Gehring, 2000), and which has limited homeotic function in flies (Berry and Gehring, 2000; Papadopoulos et al., 2012; Papadopoulos et al., 2010; Vukojevic et al., 2010), shows limited dimerization, despite being expressed in similar amounts as compared to Scr(wt) (Papadopoulos et al., 2012). Moreover, Scr(DD) dimers are largely excluded from the DNA (Fig. 2A). FCS measurements on

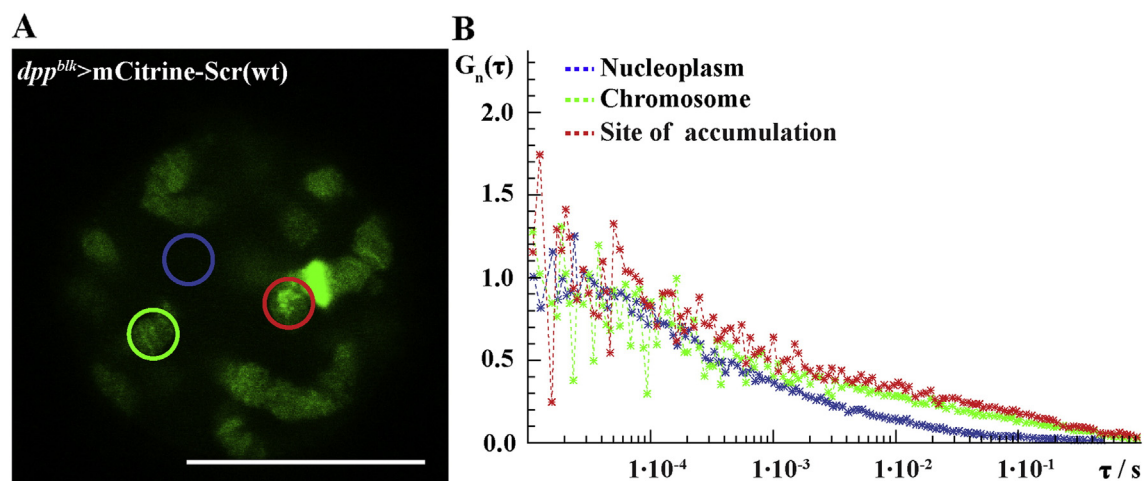


Fig. 1. Scr(wt) distribution and DNA-binding in polytene nuclei, visualized by confocal laser scanning microscopy (CLSM) and characterized by classical, single-point FCS. (A) mCitrine-Scr(wt) distribution in the salivary gland cell nucleus is non-uniform. In the nucleoplasm (blue circle) its concentration is low, on the chromosomes (green circle) it preferentially associates with sites of loose chromatin conformation, and it also forms sites of accumulation (red circle). (B) Autocorrelation curves (ACCs) normalized to the same amplitude ($G_n(\tau) = 1$ at $\tau = 1 \times 10^{-5}$ s) recorded in the areas indicated in (A) reveal fast movement of Scr(wt) in the nucleoplasm (blue ACC), as compared to the chromosome (green ACC) and the site of Scr(wt) accumulation (red ACC). The latter two indicate binding to the DNA (autocorrelation curves shifted towards longer characteristic times), but the differences between Scr(wt)–DNA binding on the chromosomes and the site of accumulation is not easily discernible. Due to bleaching, which may be extensive for FCS measurements on the chromatin, signal acquisition time on the chromosome and the site of accumulation was shorter (10 s) than for measurements in the lumen, which allow longer signal acquisition time (100 s). Scale bar is 20 μ m.

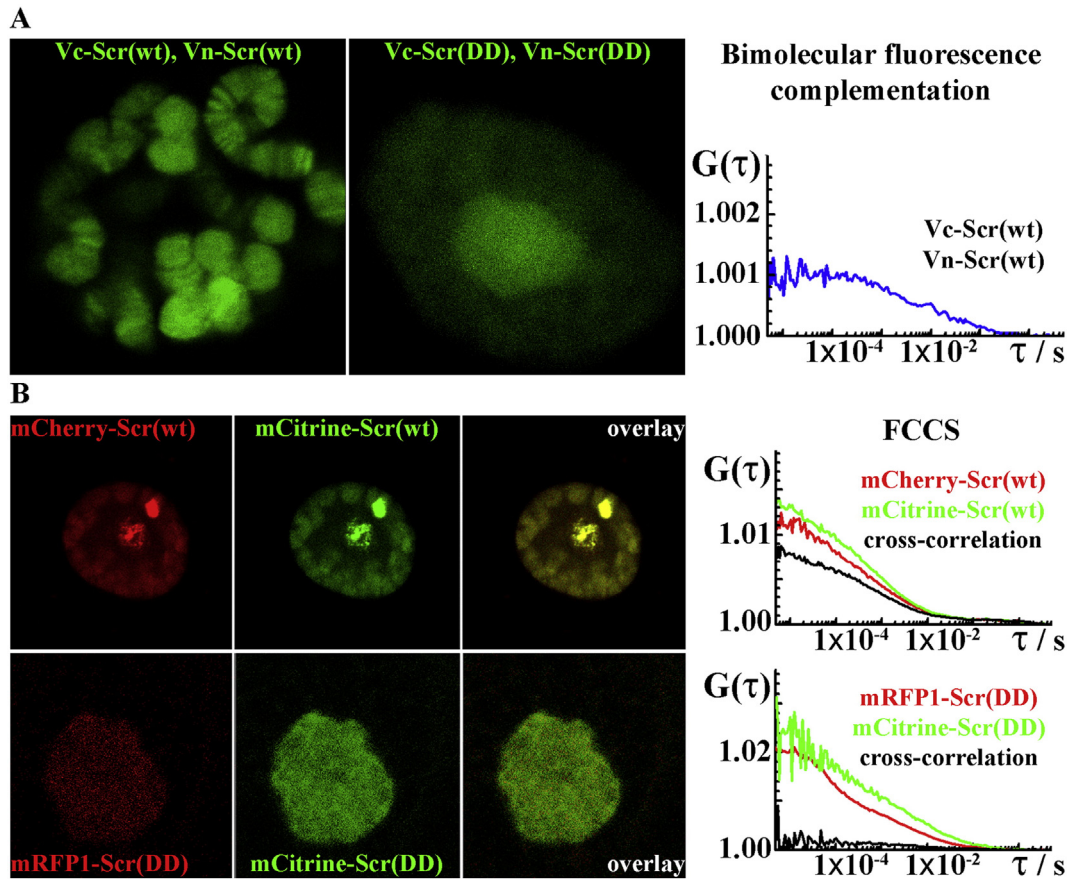


Fig. 2. Study of Scr(wt) and Scr(DD) dimer formation, visualized by CLSM and characterized by BiFC, FCS and FCCS. (A) CLSM images of Scr(wt) and Scr(DD) dimers in live salivary gland cells, visualized by BiFC. Scr(wt) dimers exhibit widespread association with chromosomal DNA, they accumulate on polytene interbands (regions of loose chromatin compaction and hence higher transcriptional activity) and are mostly excluded from the nucleoplasm. In contrast, Scr(DD) dimers show less DNA-binding activity and some accumulation at the chromocenter, but reside mostly in the nucleoplasm. Note the lower abundance of Scr(DD) dimers as compared to Scr(wt), despite their similar levels of expression. FCS measurements on Scr(wt) binding on the chromosome reveal a pronounced fraction of slowly diffusing Scr dimers, $\tau_D > 5 \times 10^{-4}$ s, and a higher contribution of components characterized with decay times $\tau_D > 1 \times 10^{-2}$ s. (B) Study of monomeric and dimeric Scr(wt) and Scr(DD) dynamics by FCCS, using dually-labeled (red and green) Scr molecules. Scr(wt) monomers (upper panel) reside on the DNA and accumulate on the giant *fkh250* binding site (and the chromocenter). Co-localization of red and green transcription factor molecules on both the *fkh250* binding site and the residual chromatin is very pronounced in this case. FCCS analysis reveals strong interaction between red and green Scr(wt) molecules (black ACC) with a relatively higher fraction of slowly diffusing molecules characterized by longer diffusion times, as compared to the individual monomers. In the case of Scr(DD) (lower panel), little, if any, binding to the DNA is observed in both the green and the red channels, and Scr is mostly excluded from chromatin [similar to (A)] and resides predominantly in the nucleoplasm. Co-localization is not observed for Scr(DD). FCCS analysis reveals little dimer formation in this case, as evidenced by the absence of significant cross-correlation (black autocorrelation curve).

Scr(wt) dimers visualized by BiFC showed multiple characteristic decay times, $\tau_D > 5 \times 10^{-4}$ s, that indicate predominantly slow diffusion. These results are corroborated by FCCS analysis, using dually labeled Scr molecules (Fig. 2B). Salivary gland nuclei of flies expressing UAS-mCherry-Scr(wt) and UAS-mCitrine-Scr(wt), as well as bearing a multimeric *fkh250* binding site [as previously described (Papadopoulos et al., 2012)], show widespread co-localization of green and red Scr monomers (Fig. 2B, upper panel), reminiscent of the binding pattern of Scr(wt) dimers tagged in the BiFC system (Fig. 2A, left). Scr(wt) dimers reside mostly on polytene chromosomes and accumulate on the introduced giant binding site (as well as the chromocenter, which contains mostly heterochromatic regions). FCCS measurements corroborated the finding that Scr(wt) forms dimers characterized by diverse mobilities, as evident from the bimodal cross-correlation curve (CCC) with at least two characteristic decay times (Fig. 2B, black). In contrast, the constitutively inactive variant Scr(DD) dimerizes to a much lower extent (compare the black CCC for Scr(wt) with the corresponding one for Scr(DD) in Fig. 2B). Moreover, Scr(DD) does not accumulate on the *fkh250* binding site or elsewhere on the chromosomes and appears to reside mostly in the nucleoplasmic space.

As evidenced by fluorescent imaging, FCS and FCCS analyses presented above, the Scr interaction pattern across the nucleus is complex. It bears various modes of residence, depending on Scr–DNA and Scr–Scr

interactions and involves three-dimensional diffusion in the nucleoplasm, specific and non-specific binding along chromosomes, as well as homodimerization on specific binding sites, but also elsewhere on the DNA. This dynamic behavior is challenging to characterize using single-point FCS measurements, which, in turn, emphasizes the need for methodology that would allow recording of molecular movement and numbers in a larger area, where spatial information is concurrently obtained. To this end, we resided to mpFCS analysis, using a prototype experimental setup that has recently been developed in our laboratory (Vitali et al., 2014 and Krmpot et al., in preparation). In mpFCS, fluorescence intensity fluctuations are recorded simultaneously using a multiplexed confocal arrangement of the illumination matrix, comprised of 1024 points, and a matrix of 1024 SPADs, thus allowing the concomitant study of molecular numbers and motion in a wider area.

We have applied this methodology to characterize the molecular distribution and dynamics of Scr(wt) and Scr(DD) dimers, tagged in the BiFC system (Fig. 3). Fig. 3A shows a salivary gland nucleus expressing Vc-Scr(wt) and Vn-Scr(wt) and bearing the *fkh250* binding site. In accordance with results obtained by CLSM and classical FCS, mpFCS analysis of the concentration and mobility of Scr(wt) dimers revealed high concentration of Scr(wt) dimers in the nucleus, as compared to the cytoplasm, where the protein is produced prior to its translocation

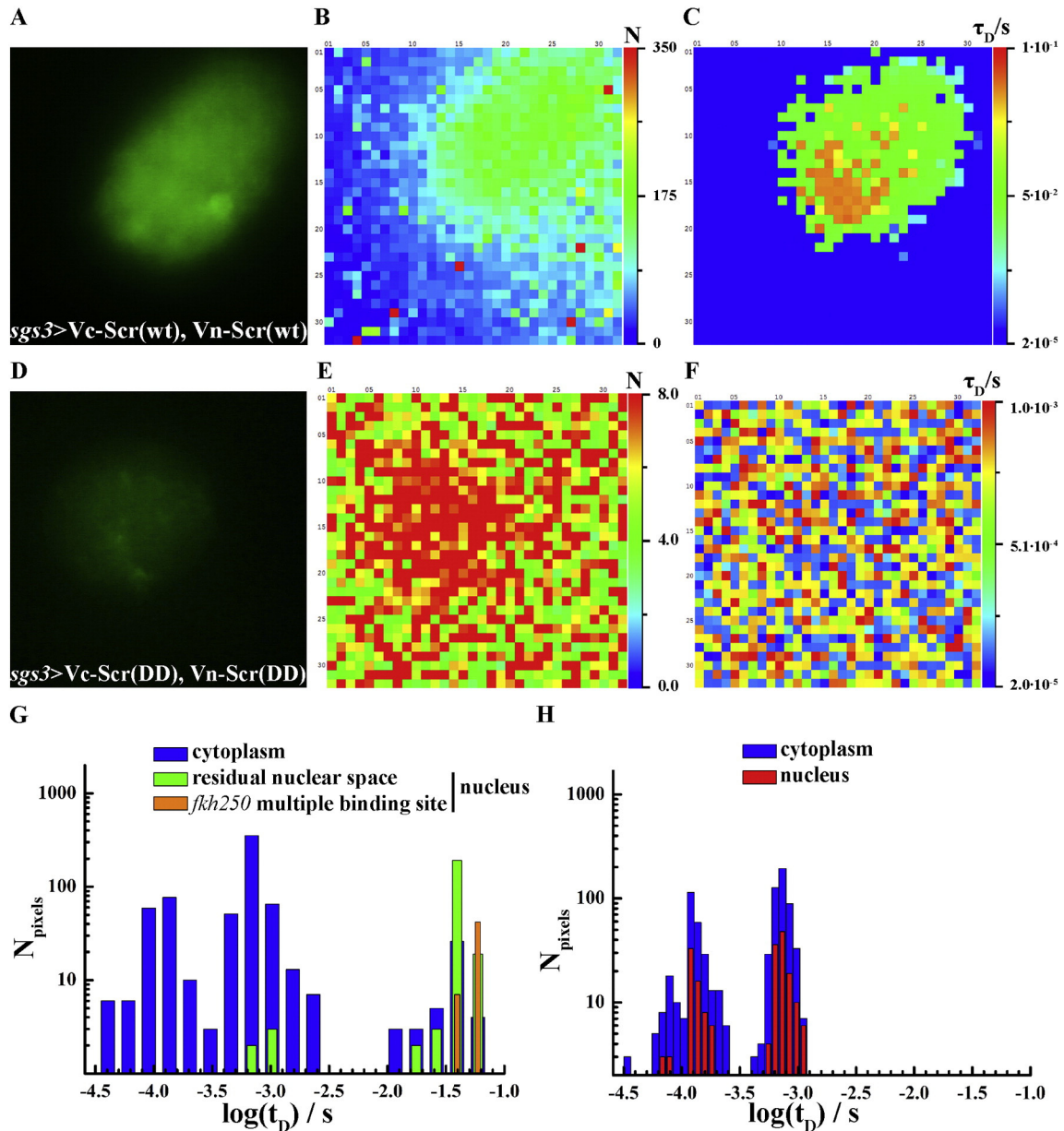


Fig. 3. Spatial distribution of molecular numbers and mobility of wild-type and constitutively inactive Scr transcription factor by mpFCS. (A) Scr(wt) dimers, visualized by BiFC and captured by the 18.0 megapixel digital single-lens reflex (DSLR) camera Canon EOS 600D (Canon Inc., Japan), associate strongly with polytene chromosomes and accumulate on the multimeric *fkh250* binding site. (B) Distribution of average molecular numbers per OVE shows high concentration of dimers in the nucleus and low concentration in the cytoplasm, the site of Scr(wt) synthesis (and possible post-translational modifications). The synthetic binding site cannot be discerned and the average number of molecules appears to be similar across the nucleus. However, the nucleus is enriched roughly 100-fold in transcription factor concentration over the cytoplasm. (C) Distribution of diffusion times in the same cell as in (A) and (B) shows different mobility of Scr(wt) molecules in the *fkh250* binding site, the residual nuclear space and the cytoplasm. Two- to three-fold differences in diffusion times are discernible between different nuclear compartments. (D) Salivary gland nuclei overexpressing Scr(DD), tagged in the BiFC system, are populated by a much lower amount of dimers, despite comparable expression levels to Scr(wt). Scr(DD) dimers do not bind significantly to the DNA and reside in the nucleoplasmic space, where they occasionally form aggregates. (E) Average molecular number distribution of Scr(DD) in the same cell as in (D) shows higher concentration of the dimers in the nucleus, as compared to the cytoplasm, but roughly 10-fold lower concentrations compared to Scr(wt) in (B). (F) The distribution of diffusion times in Scr(DD) expressing nuclei indicates that all molecules move fast. As their movement is not impeded by interactions with nuclear DNA, their movement in the nucleus is as fast as in the cytoplasm. Therefore, in the map of diffusion times the nucleus is not detectable. (G–H) Histogram of the distribution of diffusion times in Scr(wt) (G) and Scr(DD) (H) expressing nuclei. In the case of Scr(wt), the diffusion times of cytoplasmic molecules are lower than the ones in the nucleus. Within the nucleus, most of the molecules move slowly, but it is possible to discern differences in diffusion, which may reflect differences in interactions with the DNA. Scr(DD) molecules show a narrower distribution of fast diffusion times. In this case, there is barely any differences observed between nucleus and cytoplasm.

to the nucleoplasm. Concentration of Scr(wt) dimers in the nucleus was estimated to be in the micromolar range, but obvious differences in the distribution of molecular numbers were not observed (Fig. 3B). However, we observed differences in the mobility of Scr(wt) dimers between the nucleus and the cytoplasm, as well as locally within the nucleus (Fig. 3C and G). Their distribution in the nucleus is overall characterized by slow diffusion, but local differences in their mobility between the

fkh250 binding site and elsewhere on the chromosomes were observed (Fig. 3C and G). This suggests that interactions between Scr(wt) dimers and the chromatin are slow but not uniform. They are of different strength at different nuclear locations, which is reflected as differences in mobility.

In contrast, dimers of the inactive variant Scr(DD) show a very different behavior. Since they bind DNA to a lower extent, they reside

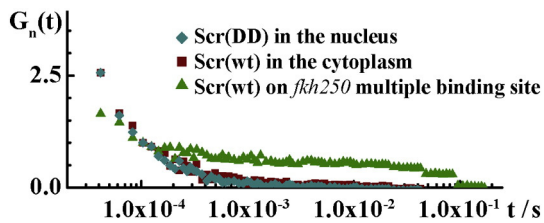


Fig. 4. Average ACCs from selected pixels (refer to Fig. S1) in nuclei expressing Scr(wt) and Scr(DD) normalized to the same amplitude ($G_n(\tau) = 1$ at $\tau = 1 \times 10^{-4}$ s). Scr(DD) molecules in the nucleus (blue diamonds) show overlapping dynamics with cytoplasmic Scr(wt) transcription factor (wine squares), which does not bind DNA. Scr(wt) molecules in the nucleus (green triangles) show significantly slower dynamics, due to interaction with the DNA.

mostly in the nucleoplasm, in between chromosomes, where they rather form aggregates (Fig. 3D). Moreover, the *fkh250* binding site is not populated by Scr(DD) dimers. mpFCS analysis of Scr(DD) dimers revealed a ten-fold lower concentration than Scr(wt) (Fig. 3E, as compared to Fig. 3B), with the nucleus being barely distinguishable over the cytoplasm in the plot of molecular numbers (Fig. 3E). The diffusion times were distributed indiscriminately between the nucleus and cytoplasm (Fig. 3F and H, as compared to Fig. 3C and G), indicating fast molecular movement and limited association with the DNA.

FCS measurements on Scr(wt)- and Scr(DD)-expressing cells showed similar dynamics between Scr(DD) and the cytoplasmic fraction of Scr(wt), which is not binding to the DNA, but a clear shift to longer characteristic times could be observed in the case of nuclear Scr(wt) dimers, suggesting strong binding to the DNA (Fig. 4).

Discussion and conclusions

The problem of how the dynamic behavior of transcription factors is linked to their function is a central question in developmental biology. This question becomes even more interesting (and challenging to answer) for transcription factors that bind DNA in a relatively indiscriminate, widespread manner, such as Hox transcription factors. Most studies involving Hox transcription factors to date have focused on understanding specific and context-dependent developmental processes, such as the regulation of specific downstream genes involved in morphogenesis. The major reason for this is presumably methodological, namely the lack of technology that could allow the study of the dynamic behavior of these proteins in live cells, such as DNA-binding, target identification, complex formation with cofactors and kinetic behavior. However, it is precisely this knowledge that would allow us to gain a holistic view of the problem of specificity that lies in the core of Hox biology. In order to do this, live cell experimentation is primarily a requirement, as fast, dynamic processes, such as transcription factor–DNA interactions, are far more than a snapshot of transcription factor nuclear distribution, which can be investigated in a fixed cell. Second, two important questions need to be answered in order to understand how biological molecules are integrated in reaction–diffusion networks, namely how many transcription factor molecules the nucleus contains (concentration) and how fast they are moving (molecular mobility). Such information can be best gained using FCS. Moreover, since the gene expression landscape is not static, but rather dynamic, it is beneficial to be able to acquire quantitative information about the local concentration and mobility of transcription factors simultaneously across the cell nucleus. This is because the temporal changes in transcription factor–DNA occupancy, mobility, interaction with other proteins and kinetics within a small fraction of nuclear volume can be influenced by local factors outside of this volume, such as global changes in chromatin conformation and dynamics, local cofactor abundance or the presence of other regulatory molecules, which can influence transcription factor concentration and DNA-binding.

In this paper, we have taken initial steps in this direction using mpFCS measurements of Scr in giant salivary gland nuclei. By classical FCS we could not simultaneously study Scr–DNA binding on sites of accumulation versus elsewhere in the nucleus, but mpFCS allowed us to concurrently record with high spatial resolution differences in diffusion and concentration of Scr between different cellular and even nuclear compartments. mpFCS indicated that the transcription factor is rather uniformly distributed across the nucleus, but at the multimeric *fkh250* binding site Scr(wt) dimer mobility is slower compared to its diffusion in the surrounding (Fig. 3C). We attribute this to the high local concentration of specific binding sites to which Scr(wt) dimers bind. This is reflected in FCS as longer diffusion times, which indicate transcription factor “stalling” due to interactions with the binding sites.

We have also observed that mobility of Scr(wt) in the residual nuclear volume (away from the binding site) is variable (Fig. 3G), which lends evidence for the existence of diverse target sites in the genome to which Scr binds with different affinities. Possible reasons why this is so could be, apart from the binding sequence itself, also the variability in region-specific abundance of cofactors, the existence of distinct chromatin states, or the variation in the chemical properties among different nuclear compartments. In fact, the notion of high and low affinity binding of Hox transcription factors is just starting to be explored and has recently been characterized in the context of Ubx–Exd binding on enhancers of the *shavenbaby* (*svb*) gene, where clustered, low-affinity binding of Ubx–Exd complexes are required for robustness of expression (Crocker et al., 2015). Our experiments point towards the existence of such binding sites also for Scr. However, whether this observation has a functional meaning also in this case, and which regulatory sequences are bound weakly and which strongly by Scr, are questions that remain to be investigated.

BiFC, FCS, FCCS and mpFCS experiments all indicate that Scr(wt) forms dimers to a much greater extent than the functionally impaired Scr(DD) (Figs 2 and 3). Artificially induced dimerization in BiFC due to high concentration and molecular crowding of transcription factor molecules bound to neighboring sites on the DNA (S. Merabet, personal communication), is not supported by our FCCS analysis and by our previous studies of Scr homodimerization in coimmunoprecipitation experiments (Papadopoulos et al., 2012).

We observed that Scr(wt) dimers localize predominantly on and strongly interact with nuclear DNA, whereas Scr(DD) dimers are more nucleoplasmic and less abundant on chromatin. This difference between the two variants, Scr(wt) and Scr(DD), together with the requirement of Scr dimer formation for homeotic function *in vivo* (Papadopoulos et al., 2012), make it possible that phosphorylation/dephosphorylation of Scr buffers its DNA-binding capacity not only through repulsion of the flexible N-terminal arm of the homeodomain, but also by controlling its ability to homodimerize.

Finally, we observed that Scr(DD) dimers to some extent form aggregates in the nucleoplasm of salivary gland cells. We attribute this to the high molecular crowding of these variants, due to the limited free space in between polytene chromosomes in these cells.

The results reported in this study agree well with our previously published results (Papadopoulos et al., 2012; Vukojevic et al., 2010) and clearly demonstrate the potential of the newly developed methodology for quantitative characterization of fast dynamical processes in live cells. Despite these positive achievements, the results of this study should be also viewed in the light of several limitations. The first and most important limitation of the current study lies in the sensitivity of the instrumental setup. The dark count of SPADs that comprise the detector is relatively high, according to the producer's specification it is 4 kHz on the average and 2 kHz at best, which gives rise to a lower signal-to-noise ratio (SNR) than in a conventional single-point FCS instrument, where the dark count of the single detector is less than 200 Hz. Another limitation, which arises due to technical reasons, is that it is at present not possible to perform measurements that are longer than 2.7 s using the full matrix detector array. In FCS, fluorescence

intensity fluctuations are recorded over a certain period of time and statistical methods of analysis are applied to detect non-randomness in the data. The longer the measurement time, the better the statistical analysis and the less noisy the resulting ACC. However, since we could not extend the signal acquisition time beyond 2.7 s using the full size of the array, this precludes direct quantitative characterization with single-molecule sensitivity and gives rise to an experimental error in the determination of molecular numbers. Comparison between single-point FCS and mpFCS measurements obtained in a dilute aqueous suspension of quantum dots, which was used as a calibration standard (Fig. S2), shows that the amplitude measured by mpFCS is much smaller than the amplitude measured by single-point FCS (Fig. S2 and F), in line with what is expected given the high dark count of SPAD detectors comprising the matrix array. However, the diffusion time measured by both setups was largely the same, both for individual quantum dots and for quantum dot agglomerates, as evident from the overlap of ACCs normalized to the same amplitude (Fig. S2) which indicates that the size of the OVE is the same in both, the conventional single-point FCS setup and the mpFCS instrument. In order to achieve direct quantitative confocal fluorescence microscopy imaging with single-molecule sensitivity and microsecond temporal resolution, the sensitivity of the detector needs to be significantly improved. At present such technology is emerging, but it is still too rare and expensive for massive parallelization.

Finally, we should also note that imaging without scanning does not allow continuous sampling across the specimen, as there are areas between the stationary focal spots from which the signal is not collected. In the present study, the pitch of the illumination matrix in the object plane is 1.5 μm . Hence, adjacent observation volume elements in the same row/column from which the signal is recorded are separated by one OVE from which the signal is not recorded. Such arrangement was deliberately used in the current setup in order to minimize cross-talk between adjacent OVE.

Previous experimental setups have demonstrated the ability to perform FCS in a larger area by means of scanning (Balaji and Maiti, 2005; Levi et al., 2003; Vukojevic et al., 2008). Such approaches underlined the importance of obtaining quantitative information across larger areas of the same sample. However, a major concern in any scanning approach is the inability to obtain information from distant locations simultaneously. For example, in raster scanning approaches signal acquisition at the level of an individual pixel is fast, in the order of microseconds, but the acquisition of an image frame is slow, lasting more than a quarter of a second for an image frame of 512×512 pixels. Therefore the information acquired in the first and the last pixel in an image frame acquired by scanning does not reflect the same state of a fast changing dynamical system. Furthermore, transcription factors exhibit complex spatio-temporal dynamics, where molecular motion reflects diffusion in the nucleoplasm, non-specific binding with the DNA during its “search” for target sites and specific binding with presumably various affinities on the DNA. Such a complex behavior is difficult to “capture” by scanning, but the ability to perform a high number of concurrent FCS measurements holds the promise to overcome such constraints.

In spite of the limitations of currently available technologies for massive production of highly sensitive SPADs, which restrain the temporal resolution and affect the quantitative analysis in live cells, as mentioned above and detailed out in Krmpot et al., in preparation, the data presented here compellingly show that it is possible to achieve quantitative confocal imaging without scanning *via* mpFCS. This approach retains all advantages of confocal microscopy, including the ability to control depth of field, improved SNR by elimination of out-of-focus light and the capability to produce 3D reconstruction of the specimen by optical sectioning. Abolishment of scanning allows confocal microscopy imaging with significantly improved temporal resolution, being 21 μs /frame in the prototype instrument used in this study. The underlying FCS analysis provides quantitative information about the spatial distribution of molecular numbers and the mobility of molecules across the specimen. This information, which cannot be deduced from classical

fluorescence microscopy imaging, is essential for understanding how molecular interactions, which take place in a small, very well defined location, are integrated *via* molecular diffusion and transporting processes into dynamic regulatory networks.

This dataset indicates that mpFCS is a suitable method for the simultaneous recording of molecular mobility and concentration over a larger area. Therefore, it is possible to study differences in these parameters in live cells with high spatiotemporal resolution. mpFCS holds the promise of facilitating the analysis of protein interactions (and other cellular components) in heterogeneous systems, such as the precise quantification of cell-to-cell variations in protein concentration and gradients (e.g. during morphogenesis). Moreover, the high temporal resolution of mpFCS is expected to allow quantification and dynamics of faster processes, such as calcium signaling and neuronal transmission, simultaneously and across larger areas. Finally, the existing technologies of precise gene-editing methodologies and a further improvement of detector sensitivity (as discussed above) are anticipated to permit the study of protein dynamic behavior in a larger area and at endogenous levels in live cells.

Supplementary data to this article can be found online at <http://dx.doi.org/10.1016/j.mod.2015.09.004>.

Acknowledgments

We thank the Vallee Foundation for awarding Prof. Walter J. Gehring the Vallee Visiting Professorship (VVP) and gratefully acknowledge financial support from the Knut and Alice Wallenberg Foundation (grant KAW 2011.0218) and the Karolinska Institutet Research Foundation. D. K. Papadopoulos was supported by a Federation of European Biochemical Societies (FEBS) postdoctoral fellowship. A. J. Krmpot and S. N. Nikolić were supported by a stipend by the Rajko and Maj Đermanović Fund. A. J. Krmpot and S. N. Nikolić acknowledge financial support from Grants III45016 and OI171038 of the Ministry of Education, Science and Technological Development of the Republic of Serbia. We thank Milan Radosavljević, M.Sc. (Eng), for his help with hardware assembly.

References

- Affolter, M., Percival-Smith, A., Muller, M., Leupin, W., Gehring, W.J., 1990. DNA binding properties of the purified Antennapedia homeodomain. *Proc. Natl. Acad. Sci. U. S. A.* 87, 4093–4097.
- Andrew, D.J., Horner, M.A., Pettit, M.G., Smolik, S.M., Scott, M.P., 1994. Setting limits on homeotic gene function: restraint of *Sex combs* reduced activity by *teashirt* and other homeotic genes. *EMBO J.* 13, 1132–1144.
- Balaji, J., Maiti, S., 2005. Quantitative measurement of the resolution and sensitivity of confocal microscopes using line-scanning fluorescence correlation spectroscopy. *Microsc. Res. Tech.* 66, 198–202.
- Berry, M., Gehring, W., 2000. Phosphorylation status of the SCR homeodomain determines its functional activity: essential role for protein phosphatase 2A,B'. *EMBO J.* 19, 2946–2957.
- Boube, M., Hudry, B., Immarigeon, C., Carrier, Y., Bernat-Fabre, S., Merabet, S., Graba, Y., Bourbon, H.M., Cribbs, D.L., 2014. *Drosophila melanogaster* Hox transcription factors access the RNA polymerase II machinery through direct homeodomain binding to a conserved motif of mediator subunit Med19. *PLoS Genet.* 10, e1004303.
- Casares, F., Mann, R.S., 1998. Control of antennal versus leg development in *Drosophila*. *Nature* 392, 723–726.
- Chang, C.P., Shen, W.F., Rozenfeld, S., Lawrence, H.J., Largman, C., Cleary, M.L., 1995. Pbx proteins display hexapeptide-dependent cooperative DNA binding with a subset of Hox proteins. *Genes Dev.* 9, 663–674.
- Crocker, J., Abe, N., Rinaldi, L., McGregor, A.P., Frankel, N., Wang, S., Alsaawadi, A., Valenti, P., Plaza, S., Payre, F., Mann, R.S., Stern, D.L., 2015. Low affinity binding site clusters confer hox specificity and regulatory robustness. *Cell* 160, 191–203.
- Duffraisse, M., Hudry, B., Merabet, S., 2014. Bimolecular fluorescence complementation (BiFC) in live *Drosophila* embryos. *Methods Mol. Biol.* 1196, 307–318.
- Furukubo-Tokunaga, K., Flister, S., Gehring, W.J., 1993. Functional specificity of the Antennapedia homeodomain. *Proc. Natl. Acad. Sci. U. S. A.* 90, 6360–6364.
- Gehring, W.J., 1987. Homeo boxes in the study of development. *Science* 236, 1245–1252.
- Gehring, W.J., 2011. How do Hox transcription factors find their target genes in the nucleus of living cells? *Biol. Aujourd'hui* 205, 75–85.
- Gibson, G., Schier, A., LeMotte, P., Gehring, W.J., 1990. The specificities of *Sex combs reduced* and *Antennapedia* are defined by a distinct portion of each protein that includes the homeodomain. *Cell* 62, 1087–1103.

- Glicksman, M.A., Soppet, D., Willard, M.B., 1987. Posttranslational modification of neurofilament polypeptides in rabbit retina. *J. Neurobiol.* 18, 167–196.
- Hrycaj, S., Chesebro, J., Popadic, A., 2010. Functional analysis of Scr during embryonic and post-embryonic development in the cockroach, *Periplaneta americana*. *Dev. Biol.* 341, 324–334.
- Hu, C.D., Chinenov, Y., Kerppola, T.K., 2002. Visualization of interactions among bZIP and Rel family proteins in living cells using bimolecular fluorescence complementation. *Mol. Cell* 9, 789–798.
- Hudry, B., Thomas-Chollier, M., Volovik, Y., Duffraisse, M., Dard, A., Frank, D., Technau, U., Merabet, S., 2014. Molecular insights into the origin of the Hox-TALE patterning system. *Elife* 3, e01939.
- Hudry, B., Viala, S., Graba, Y., Merabet, S., 2011. Visualization of protein interactions in living *Drosophila* embryos by the bimolecular fluorescence complementation assay. *BMC Biol.* 9, 5.
- Joshi, R., Passner, J.M., Rohs, R., Jain, R., Sosinsky, A., Crickmore, M.A., Jacob, V., Aggarwal, A.K., Honig, B., Mann, R.S., 2007. Functional specificity of a Hox protein mediated by the recognition of minor groove structure. *Cell* 131, 530–543.
- Joshi, R., Sun, L., Mann, R., 2010. Dissecting the functional specificities of two Hox proteins. *Genes Dev.* 24, 1533–1545.
- Knoepfler, P.S., Kamps, M.P., 1995. The pentapeptide motif of Hox proteins is required for cooperative DNA binding with Pbx1, physically contacts Pbx1, and enhances DNA binding by Pbx1. *Mol. Cell. Biol.* 15, 5811–5819.
- Kuroiwa, A., Kloter, U., Baumgartner, P., Gehring, W.J., 1985. Cloning of the homeotic Sex combs reduced gene in *Drosophila* and in situ localization of its transcripts. *EMBO J.* 4, 3757–3764.
- Le, T., Liang, Z., Patel, H., Yu, M.H., Sivasubramanian, G., Slovitt, M., Tanentzapf, G., Mohanty, N., Paul, S.M., Wu, V.M., Beitel, G.J., 2006. A new family of *Drosophila* balancer chromosomes with a w-dfd-GMR yellow fluorescent protein marker. *Genetics* 174, 2255–2257.
- LeMotte, P.K., Kuroiwa, A., Fessler, L.L., Gehring, W.J., 1989. The homeotic gene Sex Combs Reduced of *Drosophila*: gene structure and embryonic expression. *EMBO J.* 8, 219–227.
- Levi, V., Ruan, Q., Kis-Petikova, K., Gratton, E., 2003. Scanning FCS, a novel method for three-dimensional particle tracking. *Biochem. Soc. Trans.* 31, 997–1000.
- Lewis, E.B., 1978. A gene complex controlling segmentation in *Drosophila*. *Nature* 276, 565–570.
- Lu, Q., Knoepfler, P.S., Scheele, J., Wright, D.D., Kamps, M.P., 1995. Both Pbx1 and E2A-Pbx1 bind the DNA motif ATCAATCAA cooperatively with the products of multiple murine Hox genes, some of which are themselves oncogenes. *Mol. Cell. Biol.* 15, 3786–3795.
- Mahaffey, J.W., Kaufman, T.C., 1987. Distribution of the Sex combs reduced gene products in *Drosophila melanogaster*. *Genetics* 117, 51–60.
- Mann, R.S., Chan, S.K., 1996. Extra specificity from extradenticle: the partnership between HOX and PBX/EXD homeodomain proteins. *Trends Genet.* 12, 258–262.
- Martinez-Arias, A., Ingham, P.W., Scott, M.P., Akam, M.E., 1987. The spatial and temporal deployment of Dfd and Scr transcripts throughout development of *Drosophila*. *Development* 100, 673–683.
- McGinnis, W., Krumlauf, R., 1992. Homeobox genes and axial patterning. *Cell* 68, 283–302.
- Muller, M., Affolter, M., Leupin, W., Otting, G., Wuthrich, K., Gehring, W.J., 1988. Isolation and sequence-specific DNA binding of the Antennapedia homeodomain. *EMBO J.* 7, 4299–4304.
- Otting, G., Qian, Y.Q., Billeter, M., Muller, M., Affolter, M., Gehring, W.J., Wuthrich, K., 1990. Protein–DNA contacts in the structure of a homeodomain–DNA complex determined by nuclear magnetic resonance spectroscopy in solution. *EMBO J.* 9, 3085–3092.
- Otting, G., Qian, Y.Q., Muller, M., Affolter, M., Gehring, W., Wuthrich, K., 1988. Secondary structure determination for the Antennapedia homeodomain by nuclear magnetic resonance and evidence for a helix–turn–helix motif. *EMBO J.* 7, 4305–4309.
- Panzer, S., Weigel, D., Beckendorf, S.K., 1992. Organogenesis in *Drosophila melanogaster*: embryonic salivary gland determination is controlled by homeotic and dorsoventral patterning genes. *Development* 114, 49–57.
- Papadopoulos, D.K., Resendez-Perez, D., Cardenas-Chavez, D.L., Villanueva-Segura, K., Canales-del-Castillo, R., Felix, D.A., Funfschilling, R., Gehring, W.J., 2011. Functional synthetic Antennapedia genes and the dual roles of YPWM motif and linker size in transcriptional activation and repression. *Proc. Natl. Acad. Sci. U. S. A.* 108, 11959–11964.
- Papadopoulos, D.K., Skouloudaki, K., Adachi, Y., Samakovlis, C., Gehring, W.J., 2012. Dimer formation via the homeodomain is required for function and specificity of Sex combs reduced in *Drosophila*. *Dev. Biol.* 367, 78–89.
- Papadopoulos, D.K., Vukojevic, V., Adachi, Y., Terenius, L., Rigler, R., Gehring, W.J., 2010. Function and specificity of synthetic Hox transcription factors in vivo. *Proc. Natl. Acad. Sci. U. S. A.* 107, 4087–4092.
- Passner, J.M., Ryoo, H.D., Shen, L., Mann, R.S., Aggarwal, A.K., 1999. Structure of a DNA-bound ultrathorax–extradenticle homeodomain complex. *Nature* 397, 714–719.
- Qian, Y.Q., Billeter, M., Otting, G., Muller, M., Gehring, W.J., Wuthrich, K., 1989. The structure of the Antennapedia homeodomain determined by NMR spectroscopy in solution: comparison with prokaryotic repressors. *Cell* 59, 573–580.
- Qian, Y.Q., Otting, G., Furukubo-Tokunaga, K., Affolter, M., Gehring, W.J., Wuthrich, K., 1992. NMR structure determination reveals that the homeodomain is connected through a flexible linker to the main body in the *Drosophila* Antennapedia protein. *Proc. Natl. Acad. Sci. U. S. A.* 89, 10738–10742.
- Qian, Y.Q., Resendez-Perez, D., Gehring, W.J., Wuthrich, K., 1994. The des(1–6)antennapedia homeodomain: comparison of the NMR solution structure and the DNA-binding affinity with the intact Antennapedia homeodomain. *Proc. Natl. Acad. Sci. U. S. A.* 91, 4091–4095.
- Rieckhof, G.E., Casares, F., Ryoo, H.D., Abu-Shaar, M., Mann, R.S., 1997. Nuclear translocation of extradenticle requires homothorax, which encodes an extradenticle-related homeodomain protein. *Cell* 91, 171–183.
- Rogers, B.T., Peterson, M.D., Kaufman, T.C., 1997. Evolution of the insect body plan as revealed by the Sex combs reduced expression pattern. *Development* 124, 149–157.
- Ryoo, H.D., Mann, R.S., 1999. The control of trunk Hox specificity and activity by Extradenticle. *Genes Dev.* 13, 1704–1716.
- Sambrani, N., Hudry, B., Maurel-Zaffran, C., Zouza, A., Mishra, R., Merabet, S., Graba, Y., 2013. Distinct molecular strategies for Hox-mediated limb suppression in *Drosophila*: from cooperativity to dispensability/antagonism in TALE partnership. *PLoS Genet.* 9, e1003307.
- Simicevic, J., Schmid, A.W., Gilardoni, P.A., Zoller, B., Raghav, S.K., Krier, I., Gubelmann, C., Lisacek, F., Naef, F., Moniatte, M., Deplancke, B., 2013. Absolute quantification of transcription factors during cellular differentiation using multiplexed targeted proteomics. *Nat. Methods* 10, 570–576.
- Staebling-Hampton, K., Jackson, P.D., Clark, M.J., Brand, A.H., Hoffmann, F.M., 1994. Specificity of bone morphogenetic protein-related factors: cell fate and gene expression changes in *Drosophila* embryos induced by decapentaplegic but not 60A. *Cell Growth Differ.* 5, 585–593.
- Vitali, M., Bronzi, D., Krmpot, A.J., Nikolić, S., Schmitt, F.-J., Junghans, C., Tisa, S., Friedrich, T., Vukojević, V., Terenius, L., Zappa, F., Rigler, R., 2014. A single-photon avalanche camera for fluorescence lifetime imaging microscopy and correlation spectroscopy. *IEEE J. Sel. Top. Quantum Electron.* 20, 344–353.
- Vukojevic, V., Heidkamp, M., Ming, Y., Johansson, B., Terenius, L., Rigler, R., 2008. Quantitative single-molecule imaging by confocal laser scanning microscopy. *Proc. Natl. Acad. Sci. U. S. A.* 105, 18176–18181.
- Vukojevic, V., Papadopoulos, D.K., Terenius, L., Gehring, W.J., Rigler, R., 2010. Quantitative study of synthetic Hox transcription factor–DNA interactions in live cells. *Proc. Natl. Acad. Sci. U. S. A.* 107, 4093–4098.
- Vukojevic, V., Pramanik, A., Yakovleva, T., Rigler, R., Terenius, L., Bakalkin, G., 2005. Study of molecular events in cells by fluorescence correlation spectroscopy. *Cell. Mol. Life Sci.* 62, 535–550.
- Zeng, W., Andrew, D.J., Mathies, L.D., Horner, M.A., Scott, M.P., 1993. Ectopic expression and function of the Antp and Scr homeotic genes: the N terminus of the homeodomain is critical to functional specificity. *Development* 118, 339–352.
- Zhao, J.J., Lazzarini, R.A., Pick, L., 1993. The mouse Hox-1.3 gene is functionally equivalent to the *Drosophila* Sex combs reduced gene. *Genes Dev.* 7, 343–354.
- Zhao, J.J., Lazzarini, R.A., Pick, L., 1996. Functional dissection of the mouse Hox-a5 gene. *EMBO J.* 15, 1313–1322.
- Zhou, B., Bagri, A., Beckendorf, S.K., 2001. Salivary gland determination in *Drosophila*: a salivary-specific, fork head enhancer integrates spatial pattern and allows fork head autoregulation. *Dev. Biol.* 237, 54–67.